Electronic Supplementary Information

Enhancement of Cancer-Cell-Selective Cytotoxicity by a Dicopper Complex with Phenanthrene Amide-Tether Ligand Conjugate via Mitochondrial Apoptosis

Machi Hata, Itsuki Saito, Yuki Kadoya, Yoshiki Tanaka, Yutaka, Hitomi, and Masahito Kodera*

Department of Molecular Chemistry and Biochemistry, Doshisha University, Kyotanabe, Kyoto 610-0321, Japan

*E-mail: mkodera@mail.doshisha.ac.jp

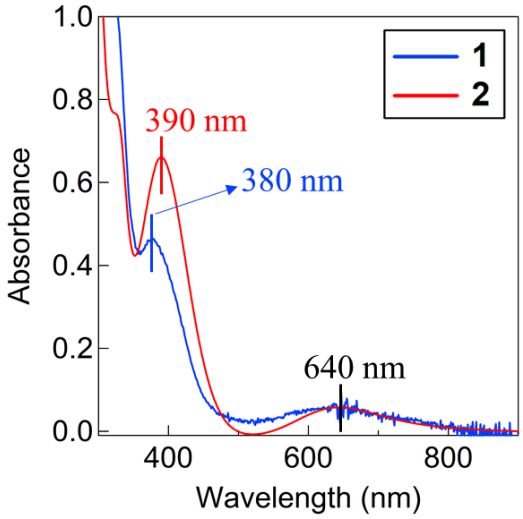

Figure S1. Electronic absorption spectra of **1** (0.25 mM) (blue) and **2** (0.25 mM) (red) in Milli-Q water at room temperature.

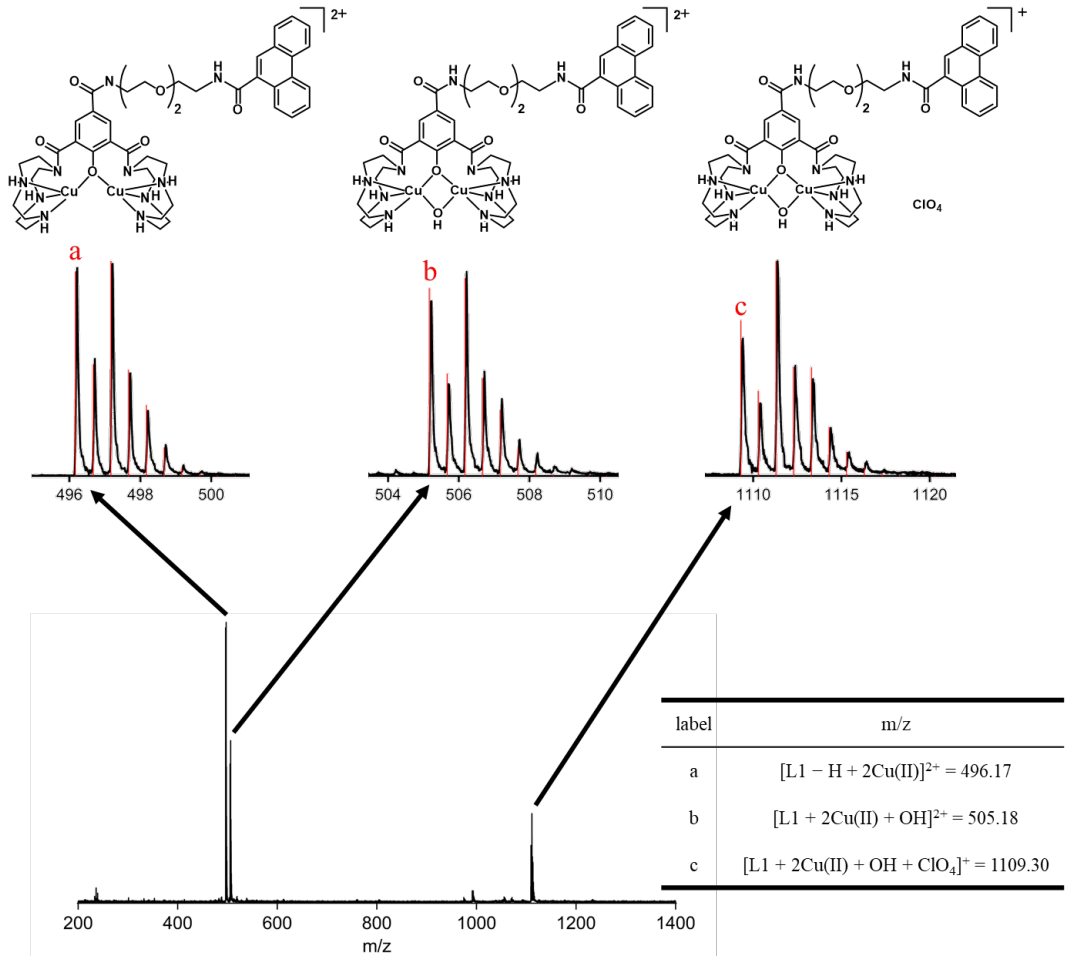

label	m/z
a	$[L1 - H + 2Cu(II)]^{2+} = 496.17$
b	$[L1 + 2Cu(II) + OH]^{2+} = 505.18$
c	$[L1 + 2Cu(II) + OH + ClO_4]^{+} = 1109.30$

Figure S2. ESI MS spectrum of **1** measured in H_2O at room temperature at orifice 1: 10 V, orifice 2: 10 V, ring lens voltage: 10 V.

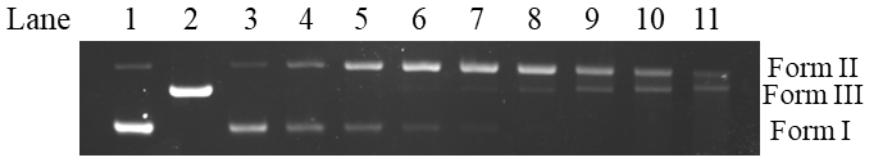

Figure S3. Agarose gel electrophoresis profile of pUC19 DNA (50 μM bp) in the presence of **1** (50 μM and H_2O_2 (500 μM) at pH 6.0. Lane 1: DNA control; lane 2: DNA with Hind III; lane 3–11: corresponded to the time of 0, 10, 20, 30, 40, 60, 120, 180, and 300 min, respectively.

Table S1. Rates (%) of Form I, Form II, and Form III in the reaction of 1 at pH 6.0

Complex (μM)	H_2O_2 (μM)	Time (min)	Form I (%)	Form II (%)	Form III (%)
50	500	0	92.2 ± 0.7	7.8 ± 0.7	-
		10	61.9 ± 2.1	38.1 ± 2.1	-
		20	25.6 ± 3.8	74.4 ± 3.8	-
		30	9.2 ± 3.1	90.8 ± 3.1	-
		40	4.7 ± 1.7	94.2 ± 1.1	1.1 ± 0.6
		60	0.0 ± 0.0	96.3 ± 0.2	3.7 ± 0.2
		120	0.0 ± 0.0	90.2 ± 3.8	9.8 ± 3.8
		180	0.0 ± 0.0	77.1 ± 4.4	22.9 ± 4.4
		300	0.0 ± 0.0	50.7 ± 2.2	49.3 ± 2.2

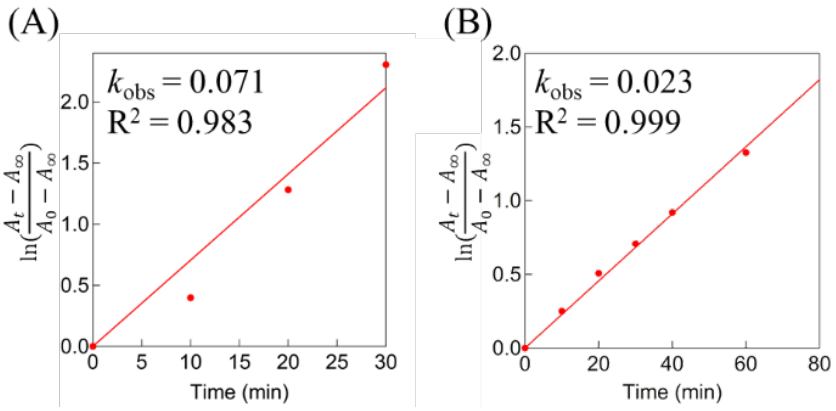

Figure S4. Pseudo-first-order plot of the decrease of Form I in the reaction of **1** (50 μM) (A) or **2** (50 μM) (B) with H_2O_2 (500 μM).

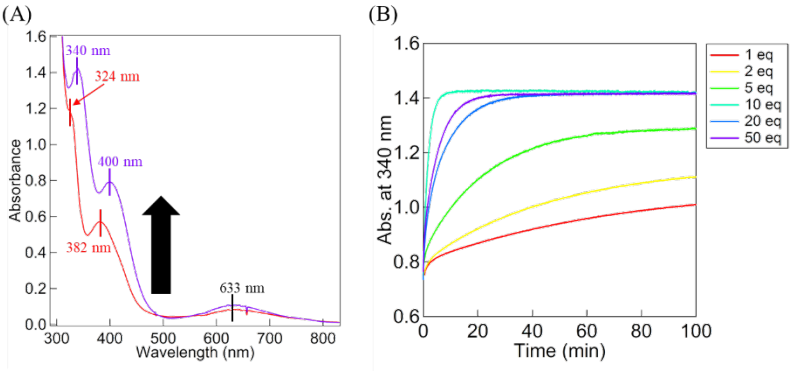

Figure S5. (A)Electronic absorption spectra of **1** (0.25 mM) (red) and hydroperoxo species **3** (purple) generated upon reaction with H_2O_2 (10 eq) in MeCN at −30°C. (B)Time courses for the formation of **3** with H_2O_2 (1–50 eq) in MeCN at −30°C, monitored at 340 nm.

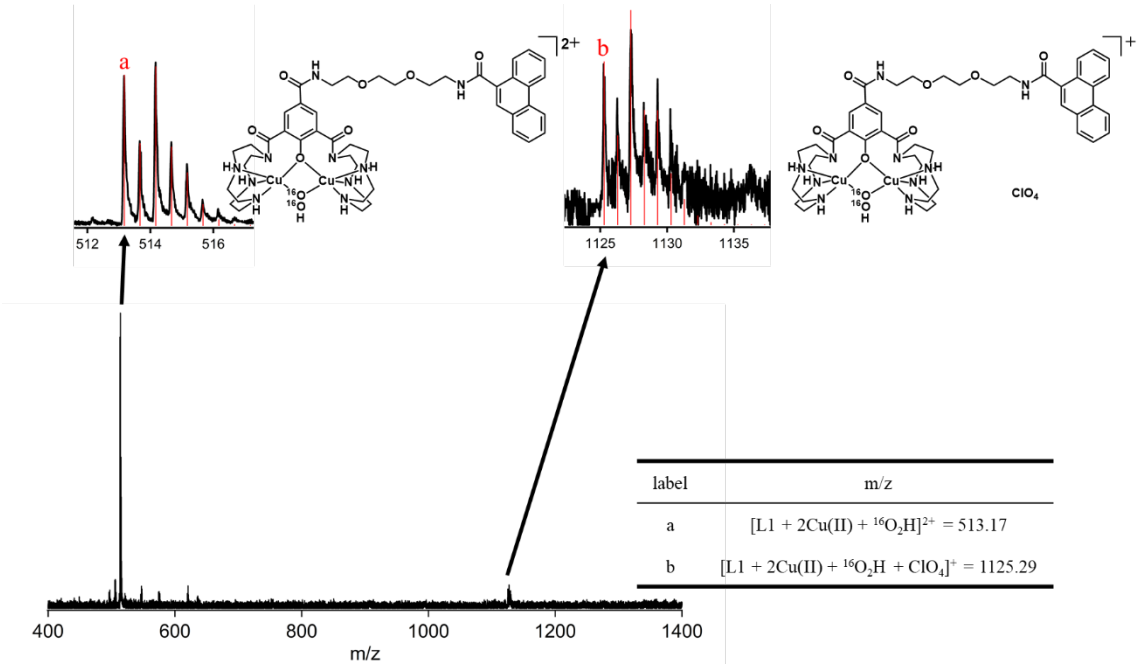

Figure S6. CSI MS spectrum of **3** formed upon reaction of **1** with $H_2{}^{16}O_2$ in H_2O at 0°C. The orifice 1: 20 V, orifice 2: 5 V, ring lens voltage: 10 V. Experimental conditions: [**1**] = 0.50 mM, [$H_2{}^{16}O_2$] = 100 mM.

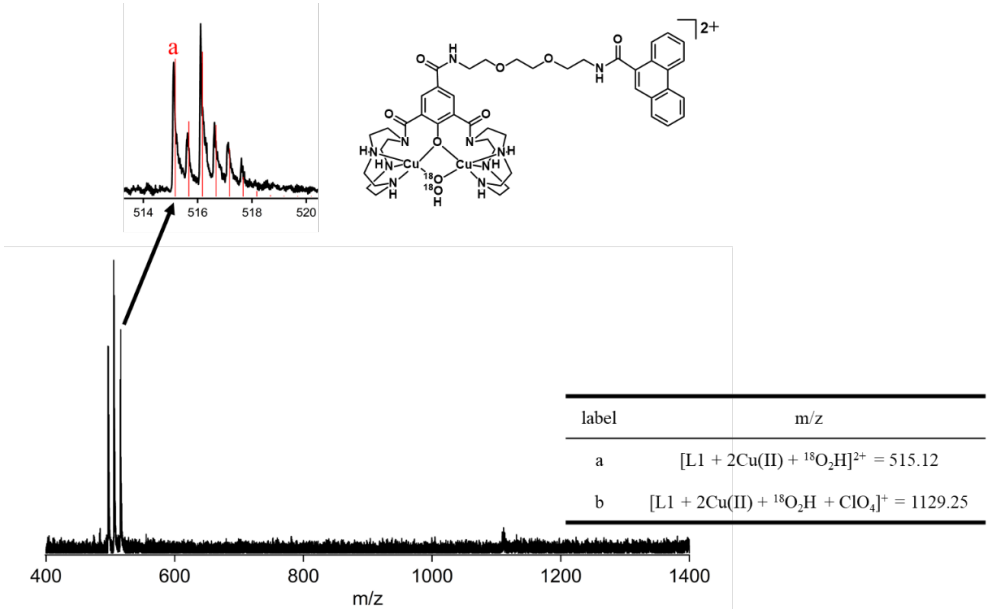

Figure S7. CSI MS spectrum of **3** formed upon reaction of **1** with $H_2{}^{18}O_2$ in H_2O at 0°C. The orifice 1: 20 V, orifice 2: 5 V, ring lens voltage: 10 V. Experimental conditions: [**1**] = 0.50 mM, [$H_2{}^{18}O_2$] = 100 mM.

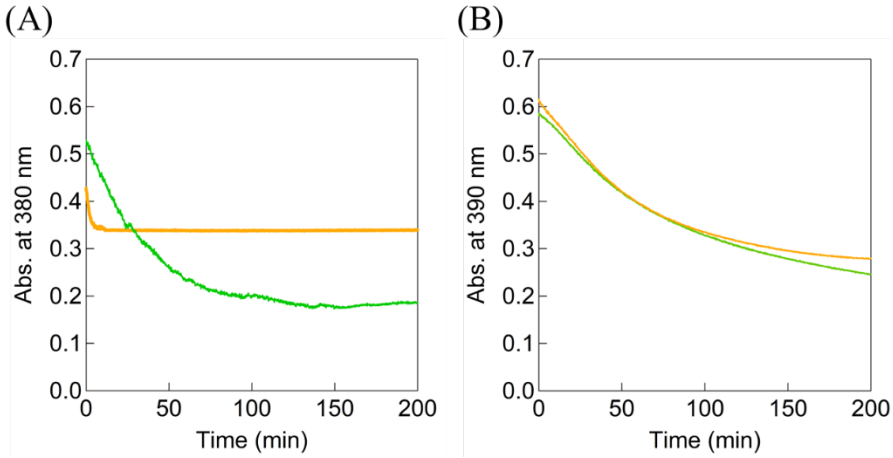

Figure S8. (A) Time courses for the decay of **3** monitored at 380 nm at room temperature in the absence (green) and presence (orange) of ct-DNA. (B) Time courses for the decay of **4** monitored at 380 nm at room temperature in the absence (green) and presence (orange) of ct-DNA. All experiments were carried out at least three times.

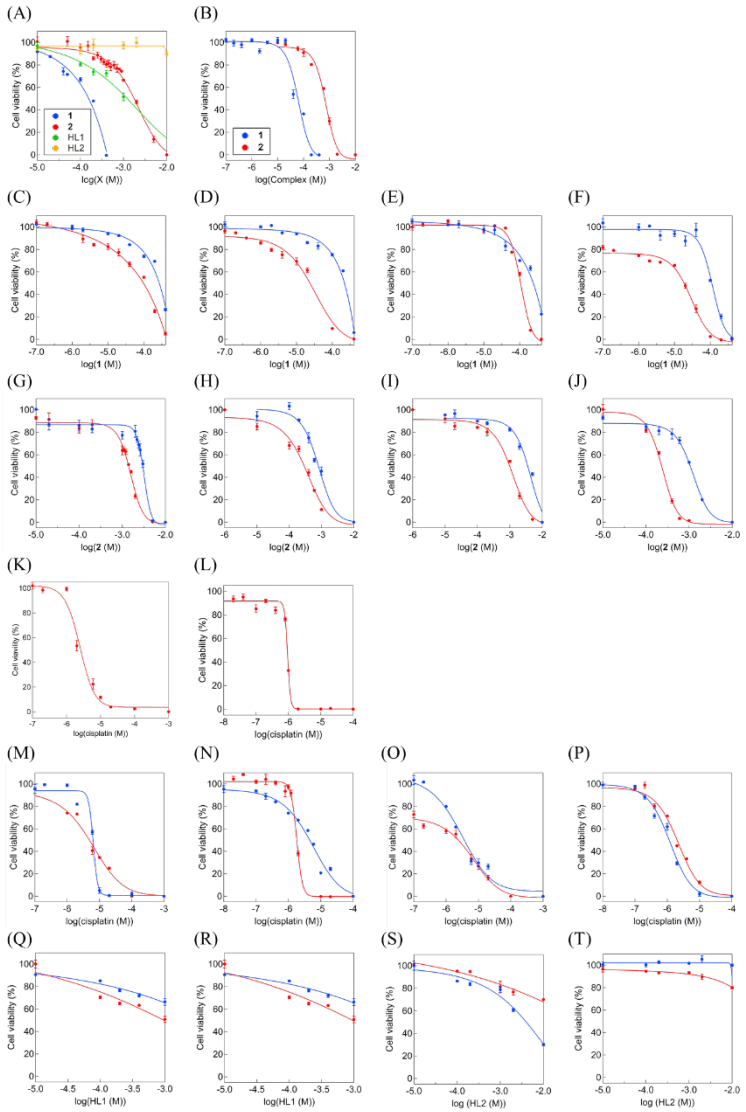

Figure S9. (A) Plots of cell viability vs log[X] (X = **1** (blue), **2** (red), HL1 (light green), and HL2 (orange)) in the MTT assay of HeLa cells treated for 24 h. (K) Plots of cell viability vs log[cisplatin] in the MTT assay of HeLa cells treated for 24 h. (B) Plots of cell viability vs log[X] (X = **1** (blue) and **2** (red)) in the MTT assay of HeLa cells treated for 48 h. (L) Plots of cell viability vs log[cisplatin] in the MTT assay of HeLa cells treated for 48 h. (C), (G), (M), (Q), (S) Plots of cell viability vs log[X] (X = **1**, **2**, cisplatin, HL1, and HL2) in the MTT assay of A549 (red) and WI-38 (blue) cells treated for 24 h. (D), (H), (N) Plots of cell viability vs log[X] (X = **1**, **2**, and cisplatin) in the MTT assay of A549 (red) and WI-38 (blue) cells treated for 48 h. (E), (I), (O), (R), (T) Plots of cell viability vs log[X] (X = **1**, **2**, cisplatin, HL1, and HL2) in the MTT assay of PK-59 (red) and 2C6 (blue) cells treated 24 h. (F), (J), (P) Plots of cell viability vs log[X] (X = **1**, **2**, and cisplatin) in the MTT assay of PK-59 (red) and 2C6 (blue) cells treated for 48 h. All experiments were carried out at least three times.

Table S2. In vitro toxicity of 1 and 2 against various cancer and normal cells by means of MTT assay (24 h)

Complex	IC_{50} (μM) (Mean ± SD)				
	Cervical	Lung		Pancreas	
	HeLa (cancer)	A549 (cancer)	WI-38 (normal)	PK-59 (cancer)	2C6 (normal)
1	156 ± 1	91.6 ± 10.0	269 ± 5	110 ± 3	238 ± 8
2	1,740 ± 110	1,430 ± 40	2,960 ± 30	1,060 ± 0	3,340 ± 10
HL1	> 1,000	> 1,000	> 1,000	> 1,000	> 1,000
HL2	> 10,000	> 10,000	> 1,000	> 10,000	> 10,000
cisplatin	2.33 ± 0.23	5.35 ± 0.82	6.33 ± 0.13	2.66 ± 0.85	3.16 ± 0.12

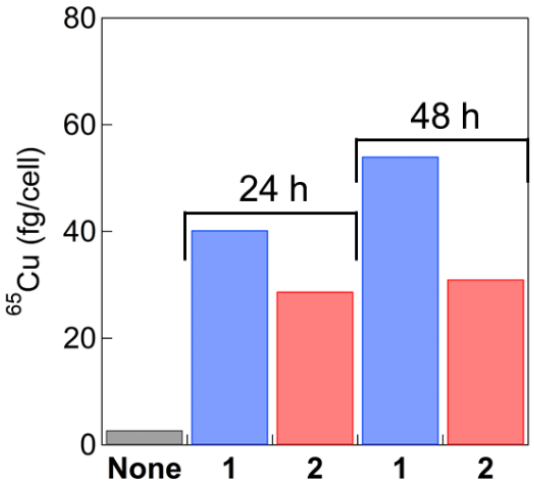

Figure S10. Cellular uptake of **1** and **2** (25 μM) in HeLa cells (2.5×10^5 cells/mL) after incubation for 24 h and 48 h.

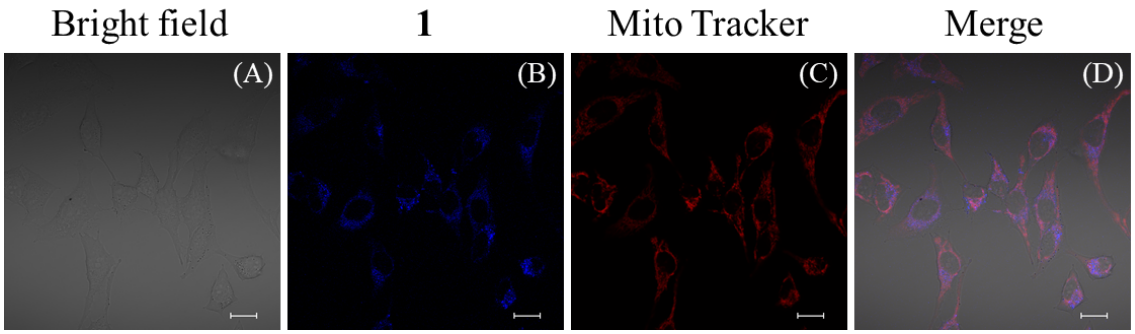

Figure S11. (A)–(D) Confocal microscopic images of **1** (200 μM) in HeLa cells on 1 h incubation in the dark. (A) Bright-field images. (B) Blue fluorescence indicates the fluorescence of **1**. (C) Red fluorescence indicates mitochondrial staining of Mitotracker Deep Red FM (50 nM) (Thermofisher). (D) Overlay images of (A)–(C). Scale bar is 20 μm.

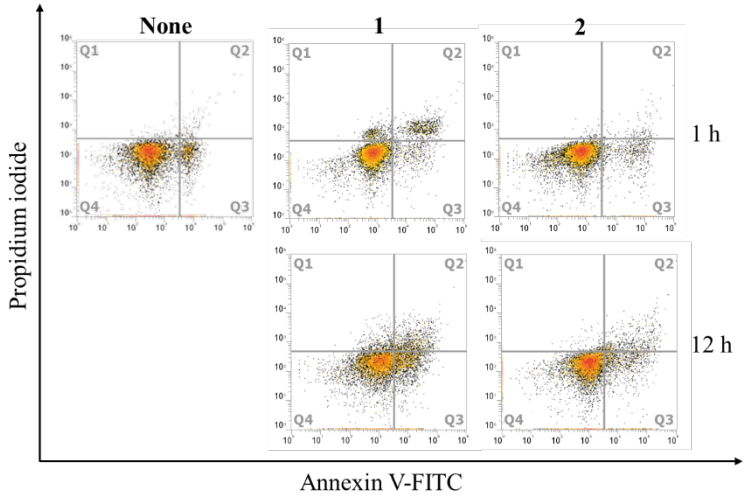

Figure S12. Induction of apoptosis by **1** and **2**. Annexin V-FITC and PI fluorescence were measured by flow cytometry. Representative dot plots of dose-dependent effect of **1** and **2** (800 μM) on apoptosis of HeLa cells treated for 1 h and 12 h. A total of 10,000 cells were collected per sample.

Table S3. Rates (%) of Induction of apoptosis by 1 and 2 against HeLa cells.

Complex	Time (h)	Rate of cells (%)			
		Q1 (FITC − /PI +)	Q2 (FITC + /PI +)	Q3 (FITC + /PI −)	Q4 (FITC − /PI −)
None		1.1	1.2	10.6	87.1
1	1	4.4	7.2	5.0	83.4
	12	5.0	8.9	18.5	67.6
2	1	0.7	1.2	8.2	89.9
	12	1.9	5.5	11.0	81.6

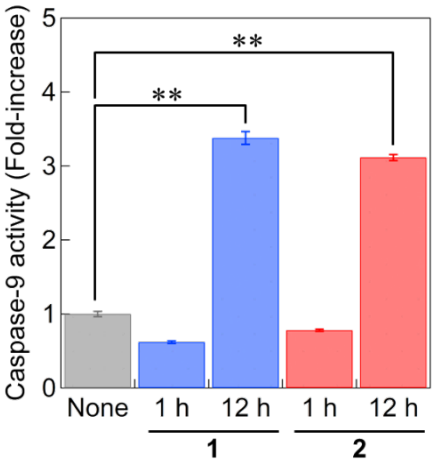

Figure S13. Caspase-9 activity in HeLa cells measured using a caspase fluorometric assay kit when treated with **1** (IC_{50}: 816 μM) (blue) and **2** (IC_{50}: 1740 μM) (red) for 1 and 12 h. Results are shown as the mean ± SD from five independent experiments. (**$p < 0.001$; two-tailed Student's t-test)

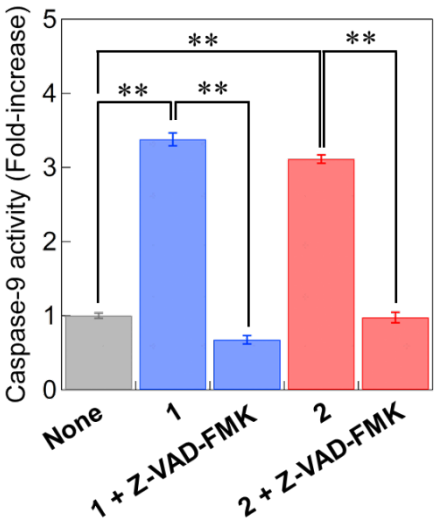

Figure S14. Caspase-9 activity in HeLa cells measured using a caspase fluorometric assay kit when treated with **1** (IC_{50}: 816 μM) (blue) and **2** (IC_{50}: 1740 μM) (red) for 12 h in the absence and the presence of Z-VAD-FMK. Results are shown as the mean ± SD from five independent experiments. (**$p < 0.001$; two-tailed Student's t-test)

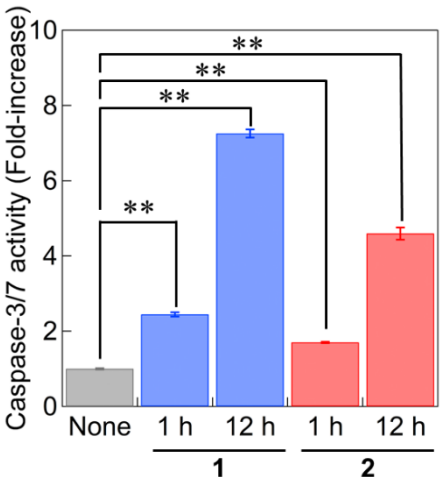

Figure S15. Caspase-3/7 activity in HeLa cells measured using a caspase fluorometric assay kit when treated with **1** (IC_{50}: 816 μM) (blue) and **2** (IC_{50}: 1740 μM) (red) for 1 and 12 h. Results are shown as the mean ± SD from five independent experiments. (**$p < 0.001$; two-tailed Student's t-test)

$$\emptyset_X = \emptyset_R \cdot \frac{A_R}{A_X} \cdot \frac{E_X}{E_R} \cdot \frac{I_{ex,R}}{I_{ex,X}} \cdot \frac{{n_X}^2}{{n_R}^2}$$

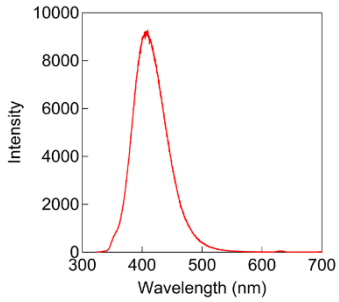

Figure S16. Emission spectra (λ_{ex} = 315 nm) of **1** (0.25 mM) in Milli-Q water at 37°C.

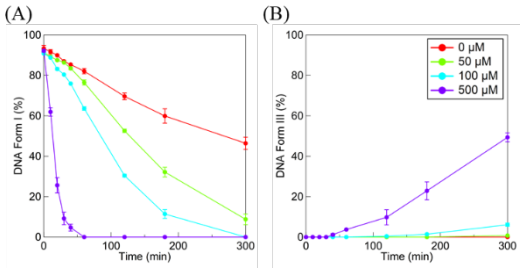

Figure S17. Time courses for the decrease of percent of Form I (A), and the increase of percent of Form III (B) upon reaction of pUC19 DNA (50 μM bp) with **1** (50 μM) in the presence of H_2O_2 (0, 50, 100, 500 μM) at pH 6.0 (MES, 10 mM) at 37°C. Experiments were carried out at least three times.

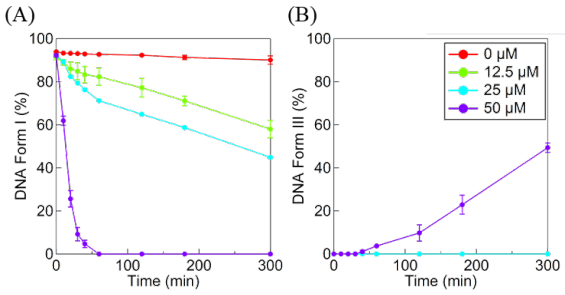

Figure S18. Time courses for the decrease of percent of Form I (A), and the increase of percent of Form III (B) upon reaction of pUC19 DNA (50 μM bp) with **1** (0, 12.5, 25, 50 μM) in the presence of H_2O_2 (500 μM) at pH 6.0 (MES, 10 mM) at 37°C. Experiments were carried out at least three times.

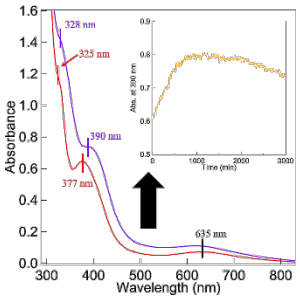

Figure S19. Electronic absorption spectra of **1** (0.25 mM) (red) and hydroperoxo species **3** (purple) generated upon reaction with H_2O_2 (200 eq) in Milli-Q water at 0°C. (inset: time courses for the formation and decay of **1** monitored at 390 nm at 0°C (orange)).

Table S4. The rate of [Cu in the cell]/[Cu in the medium during treatment]

Complex	Time (h)	[Cu in the cell]/[Cu in the medium during treatment] (%)
1	24	0.31
	48	4.38
2	24	0.16
	48	2.04